

Polymeric foams from recycled thermoplastic poly(ethylene terephthalate)

Journal of Cellular Plastics

0(0) 1–14

© The Author(s) 2020

Article reuse guidelines:

sagepub.com/journals-permissions

DOI: 10.1177/0021955X20948562

journals.sagepub.com/home/cel

Mylene S Cadete¹ , Tiago EP Gomes¹,
Pedro J Carvalho² and Victor F Neto¹

Abstract

With the increase use of plastics, there is currently a concern with the waste of materials, resulting in a series of challenges and opportunities for the waste management sector. In the present work, poly(ethylene terephthalate) (PET) foam was produced from recycled PET (RPET) from used water bottles. The recycled material was manually prepared and foamed in batches with the assistance of nitrogen gas as the physical blowing agent. RPET was characterized using Differential Scanning Calorimetry (DSC), Dynamic Mechanical Analysis (DMA), Fourier Transform Infrared Spectroscopy (FTIR) and Thermogravimetric Analysis (TGA). The influence of the pressure on the foam formation was studied and the results obtained showed that this variable influences the final product characteristics. To evaluate the behavior of the foams, their morphology, response to deformation when subject to compression and their thermal conductivities were studied. The morphology analysis showed that operating at higher-pressure results in bigger pore size but also in an increased pore size heterogeneous distribution, and foams that exhibit a higher thermal conductivity.

Keywords

PET, recycling, foam, physical process, nitrogen

¹Department of Mechanical Engineering, Center for Mechanical Technology and Automation (TEMA), University of Aveiro, Aveiro, Portugal

²Department of Chemistry, CICECO – Aveiro Institute of Materials, University of Aveiro, Aveiro, Portugal

Corresponding author:

Mylene S Cadete, Department of Mechanical Engineering, Center for Mechanical Technology and Automation (TEMA), University of Aveiro, 3810-193 Aveiro, Portugal.

Email: mylene@ua.pt

Introduction

Plastic is an important and ubiquitous material in our economy and daily lives. It has multiple functions that help tackle a number of challenges facing our society. However, too often the way plastics are produced, used and discarded fails to capture the economic benefits of a 'circular economy' approach and causes serious impacts on the environment. There is an urgent need to tackle the environmental issues that cast a long shadow over the current plastics economy.

In the European Union, the potential for recycling plastic waste remains largely unexploited. Reuse and recycling of end-of-life plastics remains very low, particularly in comparison with other materials such as paper, glass or metals.¹ Therefore, it is of utmost importance the development of products using recycled plastics. It is in this scope that the production of polymeric foam from end-of-life poly(ethylene terephthalate) (PET) raw material has been investigated.

Plastic foams have physical characteristics that are important in many applications. Its cellular structure allows much of the space in the plastic foam to be filled with air or some other gas. Given the low thermal conductivity of the gases, these foams are good thermal insulators, which enable them to be applied in insulation boards for house construction, insulation of tubes, among others.²

A wide variety of processes and techniques have been developed to enable the foaming of different resins. Synthesis and processing of polymers have shown improvements since the mid-twentieth century, when foam production methods began to be transferred from the laboratory scale to the industrial scale. Foams derived from PET were first produced in the 1990s.^{3,4}

There are numerous studies approaching chemical^{5,6} and physical methods.^{7,8} The chemical foam results from the formation of a gas through the degradation of chemicals triggered by temperature. On the physical methods a blowing agent is dissolved under pressure, directly in the fused polymer. Currently, environmentally benign gases such as supercritical carbon dioxide, CO₂, and nitrogen, N₂, are attractive alternatives as physical blowing agents because of their unique properties such as being nonflammable, nontoxic, quick dissolving, and having high self-nucleating characteristics.⁹

There are several ways of producing foams: foam extrusion, batch foaming and foam injection molding. Each technique should be used according to the foam required for the final product. However, regardless of the technology used, the foam forming principle is identical. The polymer is saturated with a blowing agent at defined pressures and temperatures. After this step, an abrupt increase in temperature or a rapid decrease in pressure causes thermodynamic instability in the saturated polymer-gas mixture, leading to the phase separation of the mixture. Cell growth and stabilization evolve as the gas diffuses into the matrix, while the foam structure gradually forms. At the end, the structure is stabilized by cooling.^{8,10,11}

Foaming by batch is a process conducted in a closed system. This process is little used at the industrial level as it is characterized by low productivity.

However, for initial design research it is useful as it allows a good control of the various variables and is a cost effective process.

Recently, more researchers have focused on the research of foamed polymer materials, where variables such as pressure, temperature, morphology, saturation time, among others, are subject of a detailed study.^{7,12,13} Tromm et al. studied the filling of the mold to determine the influence on structural morphology and uniformity of the cells using polystyrene as matrix and carbon dioxide and nitrogen as physical agents.¹⁴ A detailed characterization of the cellular structure of two types of polymeric foams, rigid polyurethane foams and cross-linked low density polyethylene foams was carried out by Pérez-Tamarit and his colleagues through non-destructive multi-scale X-ray computed micro-tomography this allow obtention of a better understanding of the connection between foaming process and cellular structure.¹⁵ Maio and Kiran examined the state of the art of the physical foaming of polymers with supercritical fluids with a primary focus on carbon dioxide. The knowledge gaps and perspectives on the foaming of all types of polymers, amorphous and semi crystalline polymers, polymer blends, copolymers and thermosetting polymers were discussed.¹⁶

Lai and his team recently published a paper presenting the production of a composite foam, using thermochemical extrusion foaming process with recycled PET, antioxidant, chain extender, blowing agent and other additives. The foam demonstrated excellent physical properties such as high mechanical performances, good thermal stabilities, small cell size, moderate antistatic capability, low density, high impact strength, where the objective is to use this material in the electronics sector.¹⁷ In thermal-acoustic insulation sector, Marques et al. reported the addition of PET residues on the production of a fire-resistant foam. In this study insulation containing 30%, 50% and 55% of PET residues were evaluated.¹⁸

In this work, we report a study on the formation of foam where the objective was to use only PET waste material as raw material, in this case obtained from used water bottles. Thus, evaluating the possibility of producing recycled PET foams without any addition of other components. A physical approach with injection of N₂ at high pressure was used. The samples used were characterized and the behavior and morphology of the foams formed at different equilibrium pressures was evaluated.

Experimental

Materials

In this work recycled PET (RPET), obtained from water bottles commercially available in the Portuguese market, was manually prepared discarding the bottom and parts containing glue from the label. Before use, all RPET samples were dried under vacuum at 373 K to prevent hydrolytic degradation.

Nitrogen (N₂) was acquired from Air Liquide with a purity of $\geq 99.999\%$.

Characterization of materials

For the foaming process to take place, the blowing agent should diffuse into the melted polymeric matrix, so it is important to study the thermal behavior of the samples. Thermal characterization of RPET was carried out by Differential Scanning Calorimeter (DSC) employing a Diamond DSC-Perkin Elmer instrument. The samples were heated from 283 K to 573 K at a ratio of 10 K/min. The melting process allows the identification of some phenomena related to changes in the structure and properties of the samples. Parameters like the glass transition temperature (T_g), melting temperature (T_m) and enthalpy of melting (ΔH_m) were measured. The percentage of crystallinity (χ_c) was estimated from the DSC results using equation (1).

$$\chi_c(\%) = \frac{[\Delta H_m]}{[\Delta H_m^o]} \times 100 \quad (1)$$

where $[\Delta H_m^o]$ is the heat of fusion of theoretical 100% crystalline PET (140 J/g).¹⁹

In order to evaluate the thermal degradation of the samples, Thermogravimetric Analysis (TGA) was carried out using the equipment Setsys Evolution 1750 Setaram in TGA mode with an S type sensor. The test in nitrogen atmosphere was operated between 298 and 1073 K with a heating rate of 10 K/min.

The study of the dynamic mechanical properties, namely the glass transition temperature, was assessed by Dynamic Thermomechanical Analysis (DMA) employing a Tritec 2000 DMA-Triton Technology. The DMA was operated in a single cantilever bending mode with the sample, contained in pocket material, subjected to heating rate of 2 K/min between 293 and 573 K, at frequencies of 1 to 10 Hz and with a strain amplitude of 0.020 mm.

By not being a virgin material, it is important to study the functional groups present in the RPET, in order to identify possible additives. The vibrational spectra were studied in the infrared region (4000 to 350 cm^{-1}) using a Bruker Tensor 27 FTIR spectrophotometer operating in absorbance mode, employing an Attenuated Total Reflectance (ATR) accessory, with a resolution of 4 cm^{-1} and performing 256 scans per spectrum. Powder samples have been used to perform this study.

Foaming process

The most widely used foam production methods are: foam extrusion, batch foaming and foam injection molding. Since the foam formation by batch is the most practical method for an initial research, this was the method used throughout this work. For the assembly of the equipment and the definition of the experimental procedure, the studies carried out by Zhong et al.²⁰ and Liu et al.²¹ were followed.

The schematic of the experimental device is shown in Figure 1. The laboratory-scale high-pressure vessel used in this process was projected in Ck45 steel with two lateral perforations, one for the vacuum connection and the other for the gas

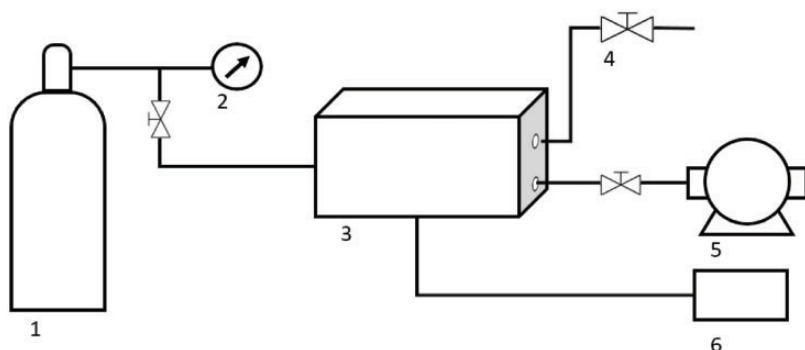


Figure 1. Schematic of the foaming process. 1 – N₂ cylinder; 2 – pressure transducer; 3 – high-pressure vessel; 4 – pressure-release valve; 5 – vacuum pump; 6 – temperature controller.

injection and depressurization. In the lower part of the cell there is an aperture for the temperature cartridge heater and one small perforation to place a type K thermocouple, with an uncertainty of 0.2 K, in order to monitor and control the reactor temperature. The procedure was described in detail elsewhere^{20,21} but the flow chart is shown in Figure 2. About 4 g of RPET flakes previously dried at 373 K under vacuum are placed inside the high pressure vessel. The procedure is started with the vacuum for 15 minutes in order to guarantee the absence of air inside the cell. After this period of time, the vacuum is switched off and the injection of gas under study pressure begins with a gradual increase in temperature until reaching 573 K. The cell is maintained at 573 K for 30 minutes and at the end of this period, it is depressurized, and the temperature is reduced to room temperature.

The system presents variables such as pressure, temperature, mass, volumetric flow, time, among others. This work was aimed at studying the behavior of the PET foam (PETFs) at three different pressures (6.5, 7.5 and 12 MPa).

Characterization of the foam

The properties of the cellular solids depend directly on the shape and structure of the cells so it is important to evaluate the morphology of the PETFs. The cell morphologies were characterized by a digital magnifying glass due to the depth of field and to determine the pore size using a Bresser MikroCamLab II software.

Compression tests were performed on a Shimadzu AGS-X-10kN mechanical testing machine, which was operated at a strain rate of 0.5 mm/min, at room temperature. It should be noted that before carrying out these tests the samples were polished in order to have parallel surfaces.

Foams are an excellent material for thermal insulation because they have unique thermal properties, such as low thermal conductivity. The determination of the thermal conductivity of the product was carried out in the Thermal Constants

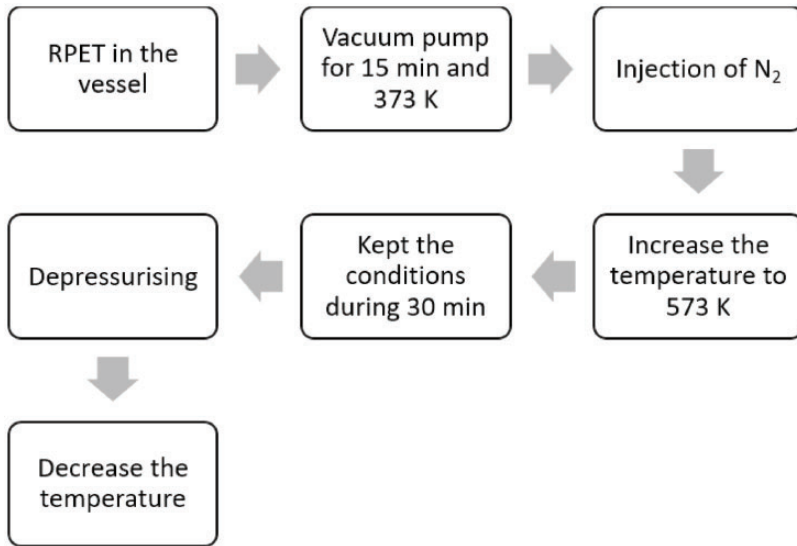


Figure 2. Flow chart of the foaming process used in this work.

Analyzer TPS 2500S-Hot Disk. The sensor used was Kapton type with 3.189 mm radius. Each measurement corresponds to 200 points operating at a power of 10 mW for 5 seconds.

Results and discussion

Characterization of the materials

From the analysis of the baseline deviations observed in the DSC thermograms, for the RPET, it was possible to determine the thermal behavior of the samples, as depicted in Figure 3.

In Figure 3, it is possible to observe a well-defined endothermic peak characteristic of the melting point, but the glass transition temperature is not evident due to the heat flux not stabilizing at the initial instants. In order to analyze the glass transition temperatures DMA analyzes were performed.

PET is well known for having very slow crystallization rate, cooling this polymer rapidly from the melt to a temperature below the transition temperature, T_g , can produce an amorphous, transparent PET. Semi-crystalline PET can be obtained by heating the solid amorphous polymer to a temperature above T_g where 30% crystallinity can be achieved.^{22,23} Using equation (1) the percentage of crystallinity present in the RPET was determined to be 30.4%, this value is in the range of expected. Torres et al. compared the thermal and mechanical properties of post-consumer poly(ethylene terephthalate) bottles with virgin resin and determined that during the first heating run appears an endothermic peak around 518.15 K,

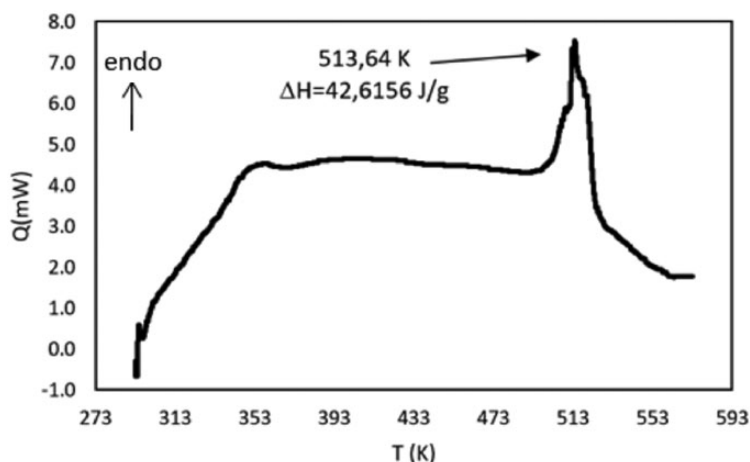


Figure 3. DSC thermogram of the RPET.

where the pellets of virgin PET exhibited 46% crystallinity and the recycled PET possess a percentage of crystallinity of 31%.²⁴ Factors such as molecular mass, the presence of nucleating agents, the degree of chain orientation, the nature of the polymerization catalyst used in the original production of PET, thermal history and cooling rate influence the crystallization of the polymer.²⁵

In the foaming process the first step consists in the dissolution of a blowing agent into the polymer matrix, but for this it is necessary the matrix to be in its melted state, making it very important to study the degradation profile of the samples. Thermogravimetry is a thermal analysis technique that studies the mass variation of the sample, as a function of temperature or time, allowing to identify the temperature range at which the sample begins to decompose.²⁶ The result obtained from the thermogravimetric analysis is graphically represented in Figure 4. The thermogram shows that in the studied RPET there is only a single decomposition step around 703 K. The RPET is shown to be thermally stable from 298 to 643 K with no significant weight loss occurring in this temperature range. The process of decomposition of the samples was observed from 643 to 733 K, where a significant loss of weight, caused by the thermal degradation of the polymer chains, was observed. Finally, at temperatures above 733 K the curve indicates a continuous and slow loss of weight up to the final temperature of 1073 K. At the end of the TGA run it was verified that in the RPET under study retained 20% of its original weight. According to the results, it is not recommended to operate a foaming process at temperatures higher than 643 K to avoid the sample degradation.

The results obtained for the dynamic mechanical analysis of the RPET are shown in Figure 5. The transition region of the material between the vitreous and the elastomeric state is characterized by the decrease of the loss modulus

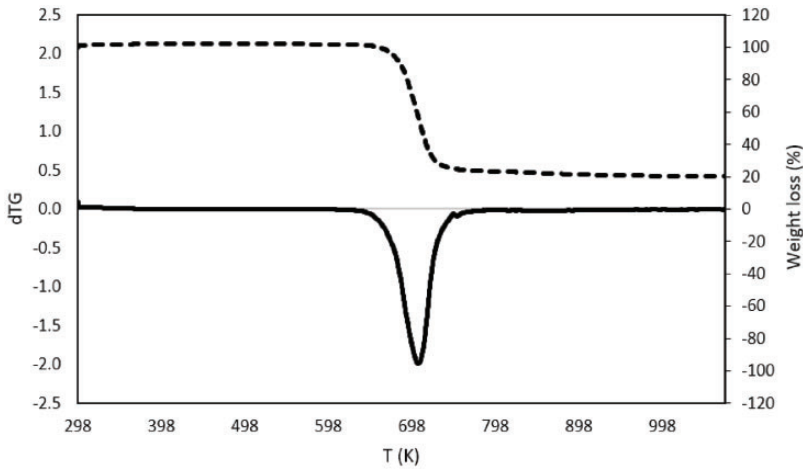


Figure 4. TGA thermogram of the RPET, dashed line represents weight loss and solid line dTG..

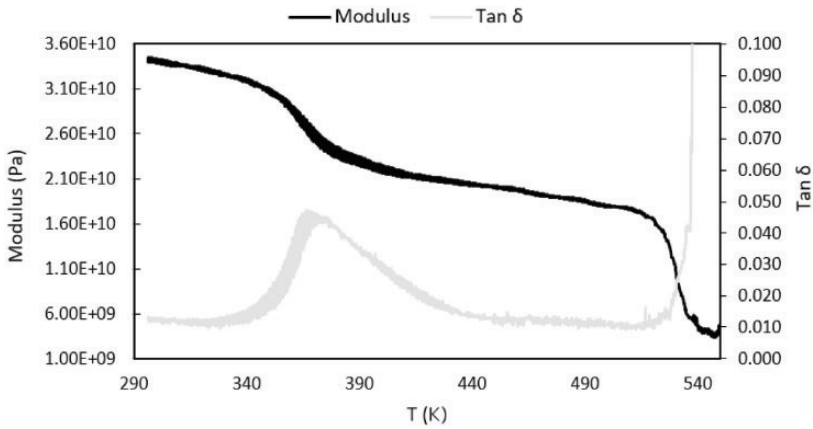


Figure 5. DMA of the RPET.

and the maximum peak of the tan delta curve. In fact, the glass transition temperatures obtained for both loss modulus and tan delta curves were relatively close to each other, but the value of the glass transition temperature, most used in the literature, corresponds to the peak of the tan delta curve.²⁷

In Figure 5(a) variation of the storage modulus between 348 and 373 K and a peak of tan δ at 371 K can be observed. It is important to note that DMA is much more sensitive than DSC and can easily measure transitions not apparent in other thermal methods.

In Figure 6, the FTIR absorbance spectrum obtained for the RPET is represented. It is possible to observe a similarity of the RPET spectrum with that of PET previously reported.^{19,20} The fact, both spectra present only the characteristic bands associated with PET structure, confirming that if additives are present it is at a very low concentration. The main absorption bands in the FTIR spectrum of PET have been assigned as follows,^{28,29} the band at 3100–2800 cm^{-1} is attributed to aromatic and aliphatic C-H bond stretching, at 1780–1650 cm^{-1} to the ester carbonyl bond stretching C=O, at 1470–1350 cm^{-1} to the bending and wagging vibrational modes of the ethylene glycol segment, at 1235 cm^{-1} to the ester group stretching, at 1090 cm^{-1} to the methylene group O-CH₂ and at 1016 and 725 cm^{-1} to aromatic bands.

Characterization of foams

In this work it was intended to evaluate the behavior of the RPET foam produced at pressures of 6.5, 7.5 and 12 MPa, and at a temperature of 573 K. There were no significant changes in the length and width of the foams, during the experiment because these dimensions were limited by the dimensions of the vessel. For each study, three samples were used. Thus, it is important to study the thickness of final product and the diameter of cell structures. With the increase in the pressure, there was a significant increase in gas uptake in all polymer samples, resulting in an increase in the diameter of the cells and in the thickness, as can be observed from Table 1. The total foam volume results from the volume of gas contained in the cells and the volume of plastic matrix, in this case PET.

The cell structures of PETFs obtained at different pressures, are exhibited in Figure 7. The increase in pressure resulted in a significant change in the foam morphology, as can be observed. Equivalent pictures were used for image analysis

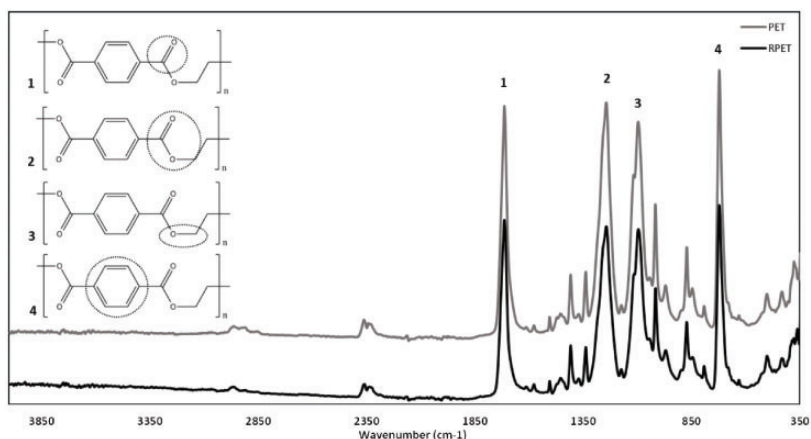
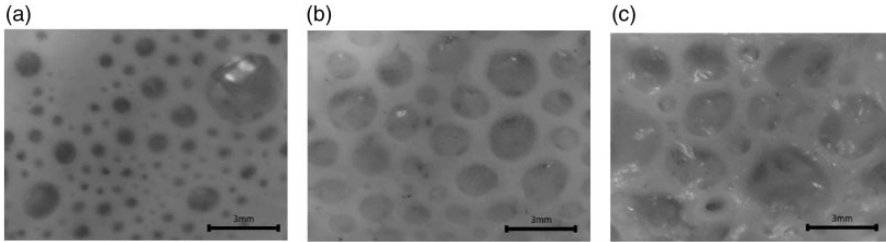


Figure 6. FTIR spectra. The PET spectrum is represented in gray and RPET in black.

Table I. Dimensions of the foams obtained at 6.5, 7.5 and 12 MPa pressures.

	6.5 MPa	7.5 MPa	12 MPa
Thickness (mm)	2.92 ± 0.05	8.25 ± 0.05	9.17 ± 0.05
Diameter (mm)	0.67 ± 0.27	1.16 ± 0.60	1.72 ± 0.98

**Figure 7.** Micrographs of PETFs obtained at different pressures: (a) 6.5 MPa; (b) 7.5 MPa; (c) 12 MPa.

(program: Bresser MikroCamLab II) to establish the pore sizes for all the samples. In all tests, the shape of the cells was approximately spherical and the cell diameter varied around 1.72 mm, 1.16 mm and 0.67 mm for the pressures of 12 MPa, 7.5 MPa and 6.5 MPa, respectively. An increase on the cell diameter with the pressure is also observed and may partly explain the observed thickness increase.

As PETFs can be applied as thermal insulation wall material or packing material, it is important to study its compression strength. The effect of saturation pressure of PETFs were studied and reported in Figure 8. Each curve represents the average of the values obtained for three samples under the same processing conditions. The cellular materials present a typical compression response comprised of three stages of deformation: linear elasticity, plateau and densification. Typically, there is an initial stage of linear elasticity at low stresses, followed by a long plastic yield zone where stresses remain for a long range of deformation values. The studied foams did not show a demarcated linear elasticity stage, which may be due mainly to the heterogeneous distribution and size of the pores in the foams produced. It is necessary to take into account that the elastic region occurs in the initial instants, where the compression tension is low, and thus, the inexistence of this region can be due to the sensitivity of the equipment.

The resulting compression-strain curve presented two well-defined regions: plateau (plastic yield) and densification. In the plastic yields the decomposition of the compressive forces in the cellular walls of the foams changing permanently, that is, the deformation is irreversible.³⁰ In this region small variations of compression induce high deformations, resulting from the collapse of most cellular pores.

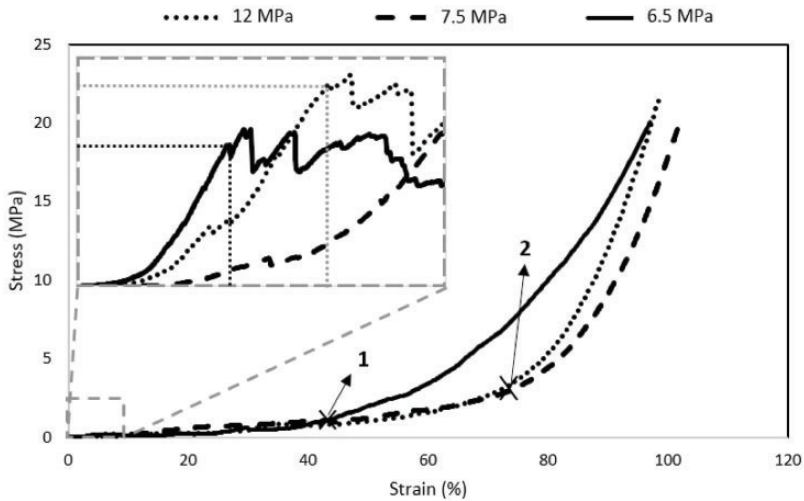


Figure 8. Compression-deformation curve.

This region is limited by the maximum deformation of 43% in the test for the samples produced at 6.5 MPa of gas pressure and 65% in the test at 12 and 7.5 MPa, with an associated maximum compression force of 1.0 MPa and 2.1 MPa, respectively.

At large, compressive strains the opposing walls of the cells crush together and the cell wall material itself is compressed.³⁰ The experimental results show compression-deformation curves with significant differences, differing in the shape of the plastic yield region in which the 6.5 MPa test is smaller. The foams obtained in the test at 12 and 7.5 MPa present a superior capacity of energy absorption due to its extensive region of plasticity when compared to foams obtained at 6.5 MPa. The differences observed in the curves are related to the anisotropy of the material observed in the characterization of the foam morphology.

Thermal conductivity expresses the amount of heat transferred per unit of time over a unit of area when a material is subjected to a temperature gradient. When it comes to insulating materials low thermal conductivity values are sought after. Factors like temperature, pressure, density of polymer, orientation of chain segments, crystal structures and degree of crystallinity influence the value of thermal conductivity of polymers.²⁴ Therefore, the value of thermal conductivity can vary in literature for the same polymers. Generally, pure polymers have low thermal conductivity, ranging from 0.1 to 0.6 W/(m·K) and for foamed polymers the values are in the order of 10^{-2} W/(m·K), which is about 10 times less than the same polymers.^{24,31} The foams obtained at 12 MPa had a thermal conductivity of 0.0756 W/(m·K) while those obtained at 7.5 MPa a smaller thermal conductivity of 0.0390 W/(m·K). Unfortunately, it was not possible to determine the thermal conductivity for the foams obtained at 6.5 MPa because the material did not

present a significant thickness for an accurate analysis. The values of thermal conductivity expressed are the result of three measurements for each type of sample.

In cellular materials such foams, the cells were produced by gas diffusion into bubbles that were nucleated or stirred into the system at the time of mixing. Their size was related to the total amount of blowing agent available. The increased amount of dissolved gas must have induced a greater thermodynamic instability and larger cell population during the foaming process. As already mentioned, one of the principal applications of polymeric foams is for thermal insulations. In this context, the heat transfer phenomena occur in three main ways: polymer conduction, gas conduction and radiation. Considering all of them, it is important to note that heat conduction through the gas in the cell interiors corresponds to the largest component of heat transfer through the foam. This type of conduction has a direct relation with the cell structure. At small cell diameters, increasing the strut fraction causes a decrease in conductivity.

Conclusions

In this work, a laboratory-scale high-pressure vessel was used for foaming recycled PET, using nitrogen as the blowing agent. The characterization of the RPET were studied by DSC, TGA, DMA, FTIR and in order to evaluate the behavior of foams the morphology, the response to deformation when exposed to compression and its associated thermal conductivity were studied.

RPET was characterized in terms of glass transition temperature, melting temperature, enthalpy of melting and crystallinity. The TGA indicates that the decomposition of RPET starts at 643 K setting that the foaming process should be operated at a lower temperature. Comparing the obtained spectrum of RPET with that typical of PET it was possible to observe a similarity in the characteristic bands. The absence of other bands confirm that additives if present are at a very low concentration.

The produced foams were characterized in terms of morphology, compression and thermal conductivity. The obtained pores of the foams demonstrated a spherical geometry with diameters increasing with the pressure increase. The cellular materials showed a typical compression response, but the studied foams did not show a demarcated linear elasticity stage. The low elasticity of the material translates thus, into a product that easily undergoes to permanent deformation. Finally, the foams were characterized by low values of thermal conductivity which favors its use as thermal insulation materials.

Acknowledgements

The authors acknowledge Lifepoly (Oiã, Portugal) for providing the recycled PET material, Ana Caço for the DSC, DMA and TGA characterizations, Celeste Azevedo for the FTIR spectroscopy, Ricardo Beja for the compression-deformation tests and Ana Barros for her

valuable advices. We thank João A.P. Coutinho for provided insight and expertise that greatly assisted the research.

Declaration of conflicting interests

The author(s) declared no potential conflicts of interest with respect to the research, authorship, and/or publication of this article.

Funding

The author(s) disclosed receipt of the following financial support for the research, authorship, and/or publication of this article: This work was supported by TEMA under the project UID/EMS/00481/2013 and project CENTRO-01-0145-FEDER-022083. P. J. Carvalho acknowledges FCT for a contract under the Investigator FCT 2015, Contract No. IF/00758/2015.

ORCID iD

Mylene S Cadete  <https://orcid.org/0000-0001-6646-2425>

References

1. European Commission. A European strategy for plastics in a circular economy. *Eur Com* 2018; Available at: <https://ec.europa.eu/environment/circular-economy/pdf/plastics-strategy-brochure.pdf> (page 6).
2. Strong AB. Foaming processes. In: Helba S (ed.) *Plastics: materials and processing*. 2nd ed. Upper Saddle River, NJ: Prentice-Hall, 2000, pp. 627–656.
3. Throne JL. *Thermoplastic foam extrusion: an introduction*. Munich: Hanser, 2004.
4. Lee S-T. Introduction. In: Lee S-T (ed.) *Foam extrusion*, 2000. Boca Raton, FL : CRC Press, Taylor and Francis.
5. Di Maio L, Coccorullo I, Montesano S, et al. Chain extension and foaming of recycled PET in extrusion equipment. *Macromol Symp* 2005; 228: 185–199.
6. Bocz K, Molnár B, Marosi G, et al. Preparation of low-density microcellular foams from recycled PET modified by solid state polymerization and chain extension. *J Polym Environ* 2019; 27: 343–351.
7. Xanthos M, Zhang Q, Dey SK, et al. Effects of resin rheology on the extrusion foaming characteristics of PET. *J Cell Plast* 1998; 34: 498–510.
8. Scamardella AM, Vietri U, Sorrentino L, et al. Foams based on poly(ethylene terephthalate) nanocomposites with enhanced thermal stability. *J Cell Plast* 2012; 48: 557–576.
9. Xi Z, Zhang F, Zhong H, et al. Microcellular injection molding of in situ modified poly(ethylene terephthalate) with supercritical nitrogen. *Polym Eng Sci* 2014; 54: 2739–2745.
10. Kumar V, Waggoner M and Kroeger L. Microcellular recycled PET foams for food packaging. *Plast Recycl Sustain* 2007; 3: 1106–1128.
11. Jin FL, Zhao M, Park M, et al. Recent trends of foaming in polymer processing: a review. *Polymers (Basel)* 2019; 11: 953.
12. Gong W, Fu H, Zhang C, et al. Study on foaming quality and impact property of foamed polypropylene composites. *Polymers (Basel)* 2018; 10: 1375.

13. Ge Y, Lu J and Liu T. Analysis of bubble coalescence and determination of the bubble radius for long-chain branched poly(ethylene terephthalate) melt foaming with a pressure balanced bubble-growth model. *AIChE J* 2020; 66: 1–13.
14. Tromm M, Shaayegan V, Wang C, et al. Investigation of the mold-filling phenomenon in high-pressure foam injection molding and its effects on the cellular structure in expanded foams. *Polymer (Guildf)* 2019; 160: 43–52.
15. Pérez-Tamarit S, Solórzano E, Hilger A, et al. Multi-scale tomographic analysis of polymeric foams: a detailed study of the cellular structure. *Eur Polym J* 2018; 109: 169–178.
16. Di E and Kiran E. Foaming of polymers with supercritical fluids and perspectives on the current knowledge gaps and challenges. *J Supercrit Fluids* 2018; 134: 157–166.
17. Lai C, Yu C, Wang F, et al. Preparation of recycled polyethylene terephthalate composite foams and their feasible evaluation for electronic packages. *Polym Test* 2019; 74: 1–6.
18. Valdevino D, Luis R, Regina H, et al. Recycled polyethylene terephthalate-based boards for thermal- acoustic insulation. *J Clean Prod* 2018; 189: 251–262.
19. Wellen RMR. Effect of polystyrene on poly(ethylene terephthalate) crystallization. *Mat Res* 2014; 17: 1620–1627.
20. Zhong H, Xi Z, Liu T, et al. Integrated process of supercritical CO₂-assisted melt polycondensation modification and foaming of poly(ethylene terephthalate). *J Supercrit Fluids* 2013; 74: 70–79.
21. Liu H, Wang X, Liu W, et al. Reactive modification of poly(ethylene terephthalate) and its foaming behavior. *Cell Polym* 2014; 33: 189–212.
22. Awaja F and Pavel D. Recycling of PET. *Eur Polym J* 2005; 41: 1453–1477.
23. Bandla S, Allahkarami M and Hanan JC. Thermal crystallinity and mechanical behavior of polyethylene terephthalate. Conference Proceedings of the Society for Experimental Mechanics Series. In: *Challenges in mechanics of time-dependent materials*. Vol. 2, 2015, pp.141–146. Available at: https://doi.org/10.1007/978-3-319-06980-7_17
24. Torres N, Robin JJ and Boutevin B. Study of thermal and mechanical properties of virgin and recycled poly(ethylene terephthalate) before and after injection molding. *Eur Polym J* 2000; 36: 2075–2080.
25. Machado LDB, Matos J and do R. Análise térmica diferencial e calorimetria exploratória diferencial. In: E A (ed.) *Técnicas de caracterização de polímeros*. São Paulo: Artliber Editora Ltda, pp. 229–262 [doc in portuguese], 2004.
26. Matos J do R and Machado LDB. Análise térmica – termogravimetria. In: *Técnicas de caracterização de polímeros*. São Paulo: E, Artliber, 2004.
27. Menard KP. *Dynamic mechanical analysis: a practical introduction*. Boca Raton: CRC Press, 1999.
28. Liang C and Krimm S. Infrared spectra of high polymers: part IX. Polyethylene terephthalate. *J Mol Spectrosc* 1959; 3: 554–574.
29. Chen Z, Hay JN and Jenkins MJ. The thermal analysis of poly(ethylene terephthalate) by FTIR spectroscopy. *Thermochim Acta* 2013; 552: 123–130.
30. Gibson LJ and Ashby MF. *Cellular solids: structure and properties*. Cambridge Solid State Science Series. 2nd ed. Cambridge: Cambridge University Press, 1999.
31. Kumar PS and Janet JG. Properties of recycled polyester. In: Muthu SS (ed.) *Recycled polyester*. Berlin: Springer, 2019, pp.1–14.